Int. J. Appl. Math. Comput. Sci., 2021, Vol. 31, No. 4, 729–744
DOI: 10.34768/amcs-2021-0050

ON THE STATISTICAL ANALYSIS OF THE HARMONIC SIGNAL AUTOCORRELATION FUNCTION

SERGIUSZ SIENKOWSKI [a,*], MARIUSZ KRAJEWSKI [a]

[a] Institute of Metrology, Electronics and Computer Science
University of Zielona Góra
Szafrana 2, 65-516 Zielona Góra, Poland
e-mail: s.sienkowski@imei.uz.zgora.pl

The article presents new tools for investigating the statistical properties of the harmonic signal autocorrelation function (ACF). These tools enable identification of the ACF estimator errors in measurements in which the triggering of the measurements is non-synchronized. This is important because in many measurement situations the initial phase of the measured signal is random. The developed tools enable testing the ACF estimator of a harmonic signal in the presence of Gaussian noise. These are the formulas on the basis of which the statistical properties of the estimator can be determined, including the bias, the variance and the mean squared error (MSE). For comparison, the article also presents the ACF statistical analysis tools used in the conditions of synchronized measurement triggering, known from the literature. Operation of the new tools is verified by simulation and experimental studies. The conducted research shows that differences between the MSE results obtained with the use of the developed formulas and those attained from simulations and experimental tests are not greater than 1 dB.

Keywords: harmonic signal, autocorrelation function, bias, variance, mean squared error.

1. Introduction

The autocorrelation function (ACF) is a tool for describing the dynamic properties of signals. The main application of the ACF is in the investigation of the degree to which the value of a signal at a given moment affects the value of this signal at a certain moment in the future (Bendat and Piersol, 2010). Unlike the ACF of a random signal (noise), which tends to zero with an increase in time shifts (delays), the ACF of periodic signals lasts for all time shifts. This implies that the ACF constitutes a good tool for detecting periodic signals occurring in the presence of noise.

The ACF and its generalized counterpart in the form of the cross-correlation function have many practical applications. They are used in radio astronomy, radar technology, and radiolocation (Beck and Plaskowski, 1987; Spiesberger, 1996; Roberts, 1997; Kogan, 1998; Weber *et al*., 1997); in ionosphere scatter investigations (Nielsen and Rietveld, 2003); in the measurement of the surface velocity of materials (Zeitler, 1997), distance measurements (Hussein *et al*., 2020), and the measurements of transport delays (Kowalczyk *et al*., 2016); in anti-collision systems (Menhaj *et al*., 1998); in spectroscopy (Hołyst *et al*., 2017); in optics (Peng and Boscolo, 2016); in optical and scanning microscopy and interferometry (Kalvani *et al*., 2019); in nuclear physics and metallurgy for radioisotope measurements (Hanus, 2019); in sports and medicine (Iqbal *et al*., 2015; Stodółka *et al*., 2017; Rahman *et al*., 2018); in mathematical statistics for studying regression models (Box *et al*., 2008); in signal processing for signal frequency analysis (Vaseghi, 2008), as well as for determining the time of signal passage through a linear circuit (Zhang *et al*., 2018); in electrical engineering for investigating signal energy parameters (Chen, 2004); and in economics for analyzing the seasonality of the results and of the recurring standards in the results of time-series model analyses (Akkucuk, 2019).

Nowadays, numerous examples are observed of the application of the ACF and of its properties to the study of the discrete-time estimators of harmonic signal parameters (Cao *et al*., 2012; Martinez and Ashrafi, 2018;

*Corresponding author

Elasmi-Ksibi *et al*., 2010; Tu and Shen, 2017; Wang *et al*., 2018). Such estimators are calculated on the basis of ACF signal samples. One of such estimators is the reformed covariance for half-length autocorrelation (RC-HLA) (Sienkowski and Krajewski, 2020). The investigation of RC-HLA includes the determination of the variance of the theoretical estimator. One of the most important components of such the variance is the covariance matrix, whose elements on the main diagonal are calculated on the basis of the ACF estimator variance.

In the paper by Sienkowski and Krajewski (2020), formulas for calculating the variance of the ACF estimator under conditions of synchronized measurement triggering and synchronous sampling are given. Under these measuring conditions, the initial phase of the signal takes a constant value, e.g., equal to zero. In order to obtain the initial signal phase close to zero at each measurement repetition, the triggering of the measurements must be synchronized, e.g., by means of a clock signal (TTL) from the measured signal source (Sienkowski and Krajewski, 2018). Such a signal is connected to the digital input of the measuring device and has a frequency equal to the measured signal frequency. Then a change in the signal state at the digital input results in a measurement initialization (external triggering). It can be a single measurement or a series of measurements. For example, such a clock source is present in the Agilent 33220A functional generator used in experimental research.

Another method of triggering the measurement start (sampling) is based on the software detection of exceeding the specified voltage level by the signal. Such a method of triggering the measurement can be realized with, e.g., the Keysight 3458A sampling voltmeter. However, in practical measurements, triggering is often non-synchronized (the initial phase of the measured signal is random in each repetition of the measurement). The literature lacks a description of the tools for investigating the ACF estimator properties of a periodic signal with noise measured under random triggering measurement conditions.

Knowledge of the statistical values of the ACF estimator obtained using these tools can be helpful in determining the bias, the variance and the MSE of other estimators, e.g., frequency, amplitude, phase, which are based on the ACF and used in many measurement applications mentioned above. For such an evaluation, one can use, for example, recommendations presented in the international document JCGM (2008), which deals with the expression of measurement uncertainty (a statistical parameter that determines a measurement inaccuracy). This document includes, among other things, the laws of uncertainty propagation, which are also valid for the bias, the variance and the MSE.

In the past few years, many works presenting the results of the studies on the ACF estimators of various signal classes have been published. Attention has been focused mainly on the ACF of random signals (Bendat and Piersol, 2010). The current state of knowledge on this subject has been extensively presented in the monograph by Broersen (2006). Certain works present formulas that make it possible to determine the expected value and the variance of the ACF estimators of such signals (Broersen, 2006; Pfeifer and Deutsch, 1981; De Gooijer and Anderson, 1985). Such formulas are not comparable with those given in this paper. Moreover, in previous works the estimation of the ACF focused on a special case of this function, i.e., the mean squared value (MSV) of random signals (Lal-Jadziak and Sienkowski, 2008; 2009) or a single realization of the ACF of a sinusoidal signal without noise (Sienkowski and Kawecka, 2013). In the paper by Lal-Jadziak and Sienkowski (2009), it was shown that the variance of the MSV estimator can be calculated using moments of random variables. Moments of a random variable were also used by Sienkowski and Kawecka (2013). On this basis, the variance of the theoretical ACF was determined. However, this variance cannot be applied to comparative studies because it is not related to the samples of the ACF estimator.

The main aim of this paper is to present new tools to determine the expected value, the bias, the variance, and the mean squared error (MSE) of the ACF estimator of a harmonic signal under random triggering measurement conditions. The harmonic signal is called a sinusoidal signal. It was assumed that the sinusoidal signal occurred in the presence of Gaussian noise. This class of signal with noise is measured in radar and sonar technology (Al-Qudsi *et al*., 2017; Hague and Buck, 2019), wireless communications (Rice *et al*., 2001), and speech signal analysis (Toth and Kocsor, 2003). The next objectives of the paper are simulation and experimental verification of the developed tools.

This paper is divided into six sections. Section 2 presents a mathematical model of a sinusoidal signal disturbed by Gaussian noise. Section 3 presents the properties of the signal ACF estimator. Formulas obtained under both random and synchronized triggering measurement conditions are given for the MSE of the estimator. Sections 4 and 5 present and discuss the results of the simulation and the experimental studies, respectively. Section 6 contains the summary of the research results. Appendix related to Section 3 can be found at the end.

2. Signal model and its measurement conditions

Let $y(t)$ be the sum of a sinusoidal signal $x(t) = A\sin(2\pi ft+\varphi)$ with amplitude A, frequency f, initial phase $\varphi \in [0, 2\pi)$, and additive Gaussian noise $q(t)$ with

the zero mean value μ_q and the standard deviation σ_q. The signal $x(t)$ and the noise $q(t)$ are independent.

If $y(t)$ is uniformly sampled at the sampling frequency f_s, then its samples can be described by the following formula:

$$\mathrm{y}\,[n] = \mathrm{x}\,[n] + \mathrm{q}\,[n], \quad n = 0, \ldots, 2M-1, \tag{1}$$

where

$$\mathrm{x}\,[n] = A\,\sin\left(\omega_0 n + \varphi\right) \tag{2}$$

and q[n] are samples of the signal $x(t)$ and the noise $q(t)$, respectively. Significant relationships exist between ω_0, f, and f_s as detailed below,

$$\omega_0 = 2\pi\frac{f}{f_s}, \quad f_s = \frac{2M}{N}f, \tag{3}$$

where $\omega_0 \in (0,\, \pi)$ is the angular frequency, wherein $2M$ and N represent the number of samples and the periods of the signal $x(t)$, respectively. Let $M' = 2M$ and $\omega = \omega_0/\pi$. Then $N = M\omega$. Moreover, let us denote by $T = 1/f$ and $T_s = 1/f_s$ the signal period and the sampling period, respectively.

The analysed signal model results from the general measurement models based on pointwise observations (Uciński, 2000). For the assumed signal model, the following combinations of measurement conditions were considered:

- synchronized triggering measurement conditions and synchronized or non-synchronized sampling,
- random triggering measurement conditions and synchronized or non-synchronized sampling.

Random triggering measurement conditions implied that after each measurement repetition, the samples y[n] in the measurement window had a different/new initial phase φ. Synchronized triggering measurement conditions implied that after each measurement repetition a set of samples y[n] had the same initial phase φ. Synchronized sampling means that $M'\,T_s = N\,T$ (where N and M' refer to natural numbers). For example, if $M = 100$ and $\omega = 0.02$, then $M' = 200$ and $N = M\omega = 2$. This means that sampling is synchronized. If, however, $\omega = 0.021$, then $N = 2.1$ and sampling is non-synchronized. Examples of measurements carried out under synchronized triggering measurement conditions are presented by Sienkowski and Krajewski (2018). Section 5 presents examples of measurements carried out under random triggering measurement conditions. Both articles also considered different signal sampling conditions.

3. Signal ACF and its properties

Let $R_s(\tau)$ represent the ACF of the signal $s(t)$ occurring in the form of a periodic signal, a random signal (noise), or a sum of both of these types of signals. Samples of the ACF of the signal $s(t)$ can be determined by using the following formula:

$$\tilde{\mathrm{R}}_{\mathrm{s}}\,[k] = \frac{1}{M}\sum_{n=0}^{M-1} \mathrm{s}\,[n]\,\mathrm{s}\,[n+k], \quad k = 0, \ldots, M-1. \tag{4}$$

Formula (4) is an estimator of the ACF calculated on the basis of the samples s[n] of the signal $s(t)$ and of the samples s[$n+k$] of the signal $s(t+\tau)$ delayed by time τ (Bendat and Piersol, 2010).

The mean squared error (MSE) of the estimator (4) can be determined as follows:

$$\mathrm{MSE}\left[\tilde{\mathrm{R}}_{\mathrm{s}}\,[k]\right] = \mathrm{Var}\left[\tilde{\mathrm{R}}_{\mathrm{s}}\,[k]\right] + \mathrm{b}_{\mathrm{s}}^2\left[\tilde{\mathrm{R}}\,[k]\right]. \tag{5}$$

This error results from the bias

$$\mathrm{b}\left[\tilde{\mathrm{R}}_{\mathrm{s}}\,[k]\right] = \mathrm{E}\left[\tilde{\mathrm{R}}_{\mathrm{s}}\,[k]\right] - R_s\,(k\cdot T_s) \tag{6}$$

and the variance

$$\mathrm{Var}\left[\tilde{\mathrm{R}}_{\mathrm{s}}\,[k]\right] = \mathrm{E}\left[\tilde{\mathrm{R}}_{\mathrm{s}}^2\,[k]\right] - \mathrm{E}^2\left[\tilde{\mathrm{R}}_{\mathrm{s}}\,[k]\right] \tag{7}$$

of the estimator, where E[$\cdot$] is the expected value operator. The bias (6) and the variance (7) are the systematic and the random components of error (5), respectively. The method of determining the error (5) is consistent with JCGM (2008). It should be noted that there are also other ways of determining estimation errors based on bootstrap (Grzegorzewski *et al.*, 2020) and Monte Carlo methods (Tagade and Choi, 2017; Krajewski, 2018), among others.

Assume that $s(t)$ is the signal $x(t)$. If the signal $x(t)$ is measured under synchronized triggering measurement conditions, then the substitution of (2) in (4) yields the following formula (Sienkowski and Krajewski, 2020):

$$\begin{aligned}\tilde{\mathrm{R}}_{\mathrm{x}}\,[k] &= \frac{1}{M}\sum_{n=0}^{M-1}\mathrm{x}\,[n]\,\mathrm{x}\,[n+k]\\ &= \frac{A^2}{2}\cos\left(k\omega_0\right) + \rho(k),\end{aligned} \tag{8}$$

where

$$\rho\,(k) = -\frac{A^2}{2M}\frac{\sin\left(M\omega_0\right)\cos\left((M+k-1)\omega_0 + 2\varphi\right)}{\sin\left(\omega_0\right)} \tag{9}$$

is the bias component of the estimator (8). Since

$$\begin{aligned}R_x\,(\tau) &= \frac{1}{T}\int_0^T x\,(t)\,x\,(t+\tau)\,\mathrm{d}t\\ &= \frac{A^2}{2}\cos\left(\frac{2\pi}{T}\tau\right),\end{aligned} \tag{10}$$

we have

$$\tilde{\mathrm{R}}_{\mathrm{x}}[k] = R_x(kT_s) + \rho(k). \tag{11}$$

This implies that

$$\mathrm{b}\left[\tilde{\mathrm{R}}_{\mathrm{x}}[k]\right] = \mathrm{E}\left[\tilde{\mathrm{R}}_{\mathrm{x}}[k]\right] - R_x(kT_s) = \rho(k). \tag{12}$$

From

$$\mathrm{Var}\left[\tilde{\mathrm{R}}_{\mathrm{x}}[k]\right] = \mathrm{E}\left[\tilde{\mathrm{R}}_{\mathrm{x}}^2[k]\right] - \mathrm{E}^2\left[\tilde{\mathrm{R}}_{\mathrm{x}}[k]\right] = 0 \tag{13}$$

it follows (Sienkowski and Krajewski, 2020) that

$$\begin{aligned}\mathrm{MSE}\left[\tilde{\mathrm{R}}_{\mathrm{x}}[k]\right] &= \mathrm{Var}\left[\tilde{\mathrm{R}}_{\mathrm{x}}[k]\right] + \mathrm{b}^2\left[\tilde{\mathrm{R}}_{\mathrm{x}}[k]\right] \\ &= \rho^2(k).\end{aligned} \tag{14}$$

From (12) and (13) we deduce that (8) is a biased estimator with zero variance.

The paper by Martinez and Ashrafi (2018) presents the result of calculating $\tilde{\mathrm{R}}_{\mathrm{x}}[k]$ for $\varphi = 0$ and $k = 1, \ldots, M$, according to which

$$\begin{aligned}\tilde{\mathrm{R}}_{\mathrm{x}}[k] &= \frac{1}{M}\sum_{n=1}^{M} \mathrm{x}[n]\,\mathrm{x}[n+k] \\ &= \frac{A^2}{2}\cos(k\omega_0) + \rho_0(k),\end{aligned} \tag{15}$$

where

$$\rho_0(k) = \frac{A^2}{2M}\frac{\sin((M+1)\omega_0)\cos((M+k)\omega_0)}{\sin(\omega_0)} \tag{16}$$

is the bias component of the estimator (15). This implies that

$$\mathrm{MSE}_0\left[\tilde{\mathrm{R}}_{\mathrm{x}}[k]\right] = \rho_0^2(k). \tag{17}$$

For the assumed synchronized triggering measurement conditions, one may additionally consider synchronized or non-synchronized sampling conditions. Under synchronized sampling conditions, $\sin(M\omega_0) = 0$. Consequently, $\rho(k) = 0$. This implies that the error (14) is zero for any k and φ. Thus, (8) is unbiased. At the same time, $\sin((M+1)\omega_0) \neq 0$ and $\cos((M+k)\omega_0) \neq 0$ for $k \neq \pi/(2\omega_0)$ and $k \neq \pi/(2\omega_0) + M/2$. Thus, $\rho_0(k) \neq 0$. This implies that under synchronized sampling conditions, the estimator (15) is biased. If the sampling is non-synchronized, both the estimators are biased.

If the signal $x(t)$ is measured under random triggering measurement conditions, then

$$\tilde{\mathrm{R}}_{\mathrm{x}}[k] = \frac{1}{M}\sum_{n=0}^{M-1} \mathrm{x}[n]\,\mathrm{x}[n+k] = \frac{A^2}{2}\cos(k\omega_0). \tag{18}$$

Furthermore (see Appendix),

$$\mathrm{b}\left[\tilde{\mathrm{R}}_{\mathrm{x}}[k]\right] = 0, \tag{19}$$

$$\mathrm{Var}\left[\tilde{\mathrm{R}}_{\mathrm{x}}[k]\right] = \frac{A^4}{16M^2}\frac{1-\cos(2M\omega_0)}{\sin^2(\omega_0)}. \tag{20}$$

This implies that

$$\mathrm{MSE}\left[\tilde{\mathrm{R}}_{\mathrm{x}}[k]\right] = \mathrm{Var}\left[\tilde{\mathrm{R}}_{\mathrm{x}}[k]\right]. \tag{21}$$

Note that the estimator (18) is unbiased and has a non-zero variance, and its error (21) does not depend on k and φ. Under synchronized sampling conditions, the error (21) is zero (note that $\cos(2M\omega_0) = 1$). If the sampling conditions are non-synchronized, then error (21) is non-zero and depends on the variance (20).

Assume that $s(t)$ is the signal $y(t)$. If the signal $y(t)$ is measured under synchronized triggering measurement conditions, then

$$\begin{aligned}\tilde{\mathrm{R}}_{\mathrm{y}}[k] &= \frac{1}{M}\sum_{n=0}^{M-1} \mathrm{y}[n]\,\mathrm{y}[n+k] \\ &= \tilde{\mathrm{R}}_{\mathrm{x}}[k] + \tilde{\mathrm{R}}_{\mathrm{q}}[k] \\ &\quad + \frac{1}{M}\sum_{n=0}^{M-1}(\mathrm{x}[n]\,\mathrm{q}[n+k]) \\ &\quad + \frac{1}{M}\sum_{n=0}^{M-1}(\mathrm{x}[n+k]\,\mathrm{q}[n]),\end{aligned} \tag{22}$$

where

$$\tilde{\mathrm{R}}_{\mathrm{q}}[k] = \frac{1}{M}\sum_{n=0}^{M-1} \mathrm{q}[n]\,\mathrm{q}[n+k]. \tag{23}$$

The paper by Martinez and Ashrafi (2018) presents the formula

$$\begin{aligned}\mathrm{Var}_0\left[\tilde{\mathrm{R}}_{\mathrm{y}}[k]\right] &= \frac{\sigma_q^4}{M} + \frac{A^2\sigma_q^2}{M} \\ &\quad + \frac{A^2\sigma_q^2}{M^2}(M-k)\cos(2k\omega_0) \\ &= \frac{\sigma_q^4}{M} + \frac{2\sigma_q^2}{M}\left(\frac{A^2}{2}\right) \\ &\quad + \frac{2\sigma_q^2}{M^2}(M-k)\left(\frac{A^2}{2}\cos(2k\omega_0)\right)\end{aligned} \tag{24}$$

making it possible to calculate the error

$$\mathrm{MSE}_0\left[\tilde{\mathrm{R}}_{\mathrm{y}}[k]\right] = \mathrm{Var}_0\left[\tilde{\mathrm{R}}_{\mathrm{y}}[k]\right] \tag{25}$$

of estimator $\tilde{\mathrm{R}}_{\mathrm{y}}[k]$ whose bias is negligibly small, in the case when $k > 0$, and $\varphi = 0$ (triggering is synchronized). The bias is omitted because for $k > 0$, the MSV that accumulates the noise information is not calculated.

Equation (24) is valid under synchronized sampling conditions. In this formula, components $A^2/2$ and $(A^2/2)\cos(2k\omega_0)$ are distinguished, which under these

sampling conditions can be obtained from (8) by calculating $\tilde{\mathrm{R}}_{\mathrm{x}}[0]$ and $\tilde{\mathrm{R}}_{\mathrm{x}}[2k]$. But the sampling need not be synchronous. Then the variance of the estimator (22) takes a new form

$$\begin{aligned}\operatorname{Var}\left[\tilde{\mathrm{R}}_{\mathrm{y}}[k]\right] &= \frac{\sigma_q^4}{M} + \frac{2\sigma_q^2}{M}\left(\frac{A^2}{2} + \rho(0)\right) \\ &\quad + \frac{2\sigma_q^2}{M^2}(M-k) \\ &\quad \left(\frac{A^2}{2}\cos(2k\omega_0) + \rho(2k)\right).\end{aligned} \tag{26}$$

where $\rho(\cdot)$ is given by (9). Equation (26) is valid for $k > 0$. It follows from the work of Lal-Jadziak and Sienkowski (2009) that, if $k = 0$, then

$$\operatorname{Var}\left[\tilde{\mathrm{R}}_{\mathrm{y}}[0]\right] = \frac{2\sigma_q^4}{M} + \frac{4\sigma_q^2}{M}\left(\frac{A^2}{2} + \rho(0)\right). \tag{27}$$

Therefore (Sienkowski and Krajewski, 2020),

$$\begin{aligned}&\operatorname{Var}\left[\tilde{\mathrm{R}}_{\mathrm{y}}[k]\right] \\ &\quad = \begin{cases} \dfrac{2\sigma_q^4}{M} + \dfrac{4\sigma_q^2}{M}\tilde{\mathrm{R}}_{\mathrm{x}}[0], & k = 0, \\ \dfrac{\sigma_q^4}{M} + \dfrac{2\sigma_q^2}{M}\tilde{\mathrm{R}}_{\mathrm{x}}[0] & \\ \quad + \dfrac{2\sigma_q^2}{M^2}(M-k)\,\tilde{\mathrm{R}}_{\mathrm{x}}[2k], & k > 0. \end{cases}\end{aligned} \tag{28}$$

As

$$\mathrm{b}\left[\tilde{\mathrm{R}}_{\mathrm{y}}[k]\right] = \begin{cases} \tilde{\mathrm{R}}_{\mathrm{x}}[0] + \sigma_q^2 - R_x(0), & k = 0, \\ \tilde{\mathrm{R}}_{\mathrm{x}}[k] - R_x(kT_s), & k > 0, \end{cases} \tag{29}$$

on the basis of (28) and (29) we obtain

$$\begin{aligned}&\operatorname{MSE}\left[\tilde{\mathrm{R}}_{\mathrm{y}}[k]\right] \\ &\quad = \begin{cases} \dfrac{2\sigma_q^4}{M} + \dfrac{4\sigma_q^2}{M}\tilde{\mathrm{R}}_{\mathrm{x}}[0] & \\ \quad + \left(\tilde{\mathrm{R}}_{\mathrm{x}}[0] + \sigma_q^2 - R_x(0)\right)^2, & k = 0, \\ \dfrac{\sigma_q^4}{M} + \dfrac{2\sigma_q^2}{M}\tilde{\mathrm{R}}_{\mathrm{x}}[0] & \\ \quad + \dfrac{2\sigma_q^2}{M^2}(M-k)\,\tilde{\mathrm{R}}_{\mathrm{x}}[2k] & \\ \quad + \left(\tilde{\mathrm{R}}_{\mathrm{x}}[k] - R_x(kT_s)\right)^2, & k > 0. \end{cases}\end{aligned} \tag{30}$$

Equations (26)–(30) are valid when sampling is synchronized or non-synchronized and the initial phase φ has any constant value in repeated measurements (triggering is synchronized). Moreover, Eqns. (28) and (29) show that (22) is a biased estimator with a non-zero variance. Equation (28) is used to investigate the properties of discrete-time algorithms for the sinusoidal signal frequency estimation (see Appendix A in the paper by Sienkowski and Krajewski (2020)).

Note that if $\varphi = 0$ for each measurement repetition and $k > 0$, then under synchronized sampling conditions, errors (25) and (30) assume the same values. Unlike (25), Eqn. (30) makes it possible to calculate the MSE irrespective of the sampling conditions. Moreover, (30) makes it possible to calculate the MSE of the MSV (the ACF estimator calculated for the delay $k = 0$).

If the signal $y(t)$ is measured under random triggering measurement conditions, then

$$\begin{aligned}\tilde{\mathrm{R}}_{\mathrm{y}}[k] &= \tilde{\mathrm{R}}_{\mathrm{x}}[k] + \tilde{\mathrm{R}}_{\mathrm{q}}[k] \\ &\quad + \frac{1}{M}\sum_{n=0}^{M-1}(\mathrm{x}[n]\,\mathrm{q}[n+k]) \\ &\quad + \frac{1}{M}\sum_{n=0}^{M-1}(\mathrm{x}[n+k]\,\mathrm{q}[n]).\end{aligned} \tag{31}$$

Then (see Appendix)

$$\mathrm{b}\left[\tilde{\mathrm{R}}_{\mathrm{y}}[k]\right] = \begin{cases} \sigma_q^2, & k = 0, \\ 0, & k > 0, \end{cases} \tag{32}$$

$$\begin{aligned}&\operatorname{Var}\left[\tilde{\mathrm{R}}_{\mathrm{y}}[k]\right] \\ &\quad = \begin{cases} \operatorname{Var}_0\left[\tilde{\mathrm{R}}_{\mathrm{y}}[k]\right] & \\ \quad + \dfrac{A^4}{16M^2}\dfrac{1-\cos(2M\omega_0)}{\sin^2(\omega_0)} + \dfrac{\sigma_q^4}{M}, & k = 0, \\ \operatorname{Var}_0\left[\tilde{\mathrm{R}}_{\mathrm{y}}[k]\right] & \\ \quad + \dfrac{A^4}{16M^2}\dfrac{1-\cos(2M\omega_0)}{\sin^2(\omega_0)}, & k > 0. \end{cases}\end{aligned} \tag{33}$$

On the basis of (32) and (33), we obtain

$$\begin{aligned}&\operatorname{MSE}\left[\tilde{\mathrm{R}}_{\mathrm{y}}[k]\right] \\ &\quad = \begin{cases} \operatorname{Var}_0\left[\tilde{\mathrm{R}}_{\mathrm{y}}[k]\right] + \sigma_q^4\left(1 + \dfrac{1}{M}\right) & \\ \quad + \dfrac{A^4}{16M^2}\dfrac{1-\cos(2M\omega_0)}{\sin^2(\omega_0)}, & k = 0, \\ \operatorname{Var}_0\left[\tilde{\mathrm{R}}_{\mathrm{y}}[k]\right] & \\ \quad + \dfrac{A^4}{16M^2}\dfrac{1-\cos(2M\omega_0)}{\sin^2(\omega_0)}, & k > 0. \end{cases}\end{aligned} \tag{34}$$

It follows from (32) and (33) that if $k > 0$, then (31) is an unbiased estimator with a non-zero variance. The error (34) does not depend on φ and under synchronized sampling conditions is reduced by the value of the variance (20).

To sum up, Eqns. (30) and (25) known from the literature are used under synchronized triggering measurement conditions. At the same time, formula (30) can be used when sampling is synchronized or non-synchronized. Moreover, Eqn. (30) enables the determination of the MSE of the MSV estimator. Equation (25) is used when sampling is synchronized. Under

these measurement conditions, Eqns. (30) and (25) are equivalent. Equation (30) can be used for any value of φ, while Eqn. (25) only for $\varphi = 0$. The new formula (34) is used under random triggering measurement conditions. At the same time, Eqn. (34) can be used under synchronized or non-synchronized sampling conditions. The components of the MSE are the bias and the variance. These components in the literature are described by (28) and (29) for the constant initial phase of the signal, while the paper presents new equations (32) and (33) for the random initial phase of the signal.

4. Simulation studies

In order to verify the formulas for the ACF estimator errors presented in Section 3, simulation studies were conducted, which consisted of the determination of K results of the estimation of the ACF $R_s(\tau)$ of the signal $s(t)$ and of the calculation of the following error:

$$\tilde{\mathrm{M}}\mathrm{SE}\left[\tilde{\mathrm{R}}_{\mathrm{s}}[k]\right] = \frac{1}{K}\sum_{j=0}^{K-1}\left(\tilde{\mathrm{R}}_{\mathrm{s}}^{(j)}[k] - R_s(kT_s)\right)^2, \quad (35)$$

where $\tilde{\mathrm{R}}_{\mathrm{s}}^{(j)}[k]$ is the j-th result of the ACF estimation, which was obtained using (4) and the signal samples obtained under synchronized or random triggering measurement conditions and synchronized or non-synchronized sampling.

If $s(t)$ is the signal $y(t)$, then

$$\tilde{\mathrm{M}}\mathrm{SE}\left[\tilde{\mathrm{R}}_{\mathrm{y}}[k]\right] = \frac{1}{K}\sum_{j=0}^{K-1}\left(\tilde{\mathrm{R}}_{\mathrm{y}}^{(j)}[k] - R_x(kT_s)\right)^2. \quad (36)$$

The components of the error (36) are the bias

$$\tilde{\mathrm{b}}\left[\tilde{\mathrm{R}}_{\mathrm{y}}[k]\right] = \frac{1}{K}\sum_{m=0}^{K-1}\tilde{\mathrm{R}}_{\mathrm{y}}^{(m)}[k] - R_x(k\,T_s) \quad (37)$$

and the variance

$$\tilde{\mathrm{V}}\mathrm{ar}\left[\tilde{\mathrm{R}}_{\mathrm{y}}[k]\right] = \frac{1}{K}\sum_{j=0}^{K-1}\left(\frac{1}{K}\sum_{m=0}^{K-1}\tilde{\mathrm{R}}_{\mathrm{y}}^{(m)}[k] - \tilde{\mathrm{R}}_{\mathrm{y}}^{(j)}[k]\right)^2. \quad (38)$$

The simulations were carried out using the MathCAD computer program.

Firstly, the error characteristics (25), (30), (34), and (36) for a fixed M, ω (or N) and SNR (SNR $= 10\log(0.5A^2/\sigma_q^2)$), and for a changing delay k were determined. The sampling conditions were assumed to be non-synchronized. Synchronized measurement triggering was achieved by assuming $\varphi = 0$ in each repetition of the simulation (Figs. 1(a) and 1(c)). The simulation of random measurement triggering was conducted such that the phase φ of the sinusoidal signal $x(t)$ was randomized by means of a pseudo-random number generator of a uniform distribution over the [0, 2π) interval (Figs. 1(b) and 1(d)). This means that $\varphi \sim \mathrm{U}[0, 2\pi)$. Moreover, it was assumed that $A = 3\sqrt{2}$ V, $f = 50$ Hz, $\omega = 0.021$ ($N = 2.1$), $M = 100$, SNR = 20 dB, and SNR = 70 dB, $K = 1000$. For comparison, Fig. 2 also shows the test results for the bias, (29) and (32), and the variance, (28) and (33), which were compared, similarly to the MSE, with the results obtained on the basis of (37) and (38). However, in the sequel the results are limited to presenting only the results of the MSE, which combines the bias and the variance of estimator ACF. The results of the MSE obtained from Eqns. (30) and (34) presented in the following work also confirm the correctness of operations of the formulas on the bias, (29) and (32), and the variance, (28) and (33).

The values of the error (36) show that Eqns. (30) and (34) are correct. From the conducted simulations, it also follows that under non-synchronized sampling conditions, the application of (25) can signify underestimation of the MSE, irrespective of how the measurement was triggered. It is worth noticing, that the greatest difference between the relative errors (30) and (36) (for $\varphi = 0$) and (34) and (36) (for $\varphi \sim \mathrm{U}[0, 2\pi)$) does not exceed 1 dB (see the sample error values in Table 1).

The subsequent studies involved the determination of characteristics (25), (30), (34), and (36) for a fixed delay k_0 and for changing values of the SNR, M, φ, and ω (or N). The sampling conditions were assumed to be non-synchronized (this only applied to the error characteristics as a function of M, φ and SNR). The simulations were conducted for $A = 3\sqrt{2}$ V, $f = 50$ Hz, $\omega = 0.021$ ($N = 2.1$), $M = 100$, SNR = 20 dB, and SNR = 70 dB, $k_0 = 7$, $K = 1000$. Figures 3(a), 3(c), and 3(e) present the relative MSE characteristics obtained under synchronized triggering measurement conditions ($\varphi = 0$). The remaining figures present the relative MSE characteristics obtained under random triggering measurement conditions ($\varphi \sim \mathrm{U}[0, 2\pi)$). Moreover, Fig. 4 presents the relative MSE characteristics obtained under synchronized triggering measurement conditions for $\varphi \in [0, 2\pi)$.

Table 1. Sample relative error values (25), (30), (34), and (36) from Figs. 1(a) and 1(b).

MSE [dB]	φ/k	$k = 20$	$k = 50$	$k = 80$
(25)	$\varphi = 0$	–30.08	–35.18	–31.94
(30)	$\varphi = 0$	–30.21	–26.60	–23.33
(34)	$\varphi \sim \mathrm{U}[0, 2\pi)$	–17.28	–28.45	–23.50
(36)	$\varphi = 0$	–30.26	–26.74	–23.31
	$\varphi \sim \mathrm{U}[0, 2\pi)$	–17.21	–28.49	–23.43

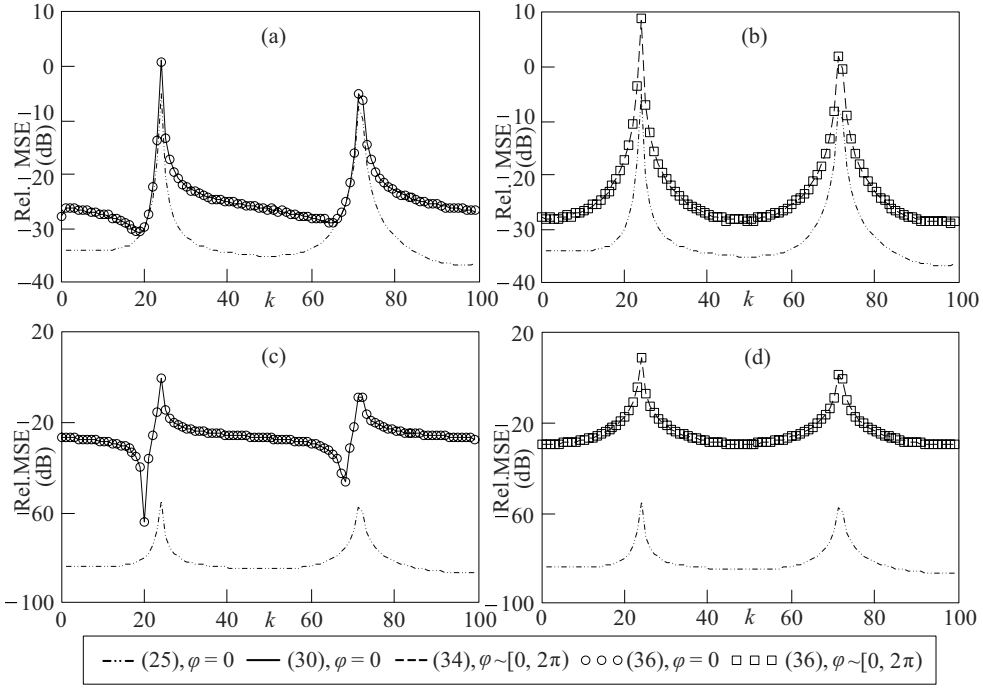

Fig. 1. Relative MSEs of the ACF estimator as a function of k for $A = 3\sqrt{2}$ V, $f = 50$ Hz, $\omega = 0.021$ ($N = 2.1$), $M = 100$, and $K = 1000$: $\varphi = 0$, SNR $= 20$ dB (a), $\varphi \sim$ U[0, 2π), SNR $= 20$ dB (b), $\varphi = 0$, SNR $= 70$ dB (c), and $\varphi \sim$ U[0, 2π), SNR $=$ 70 dB (d).

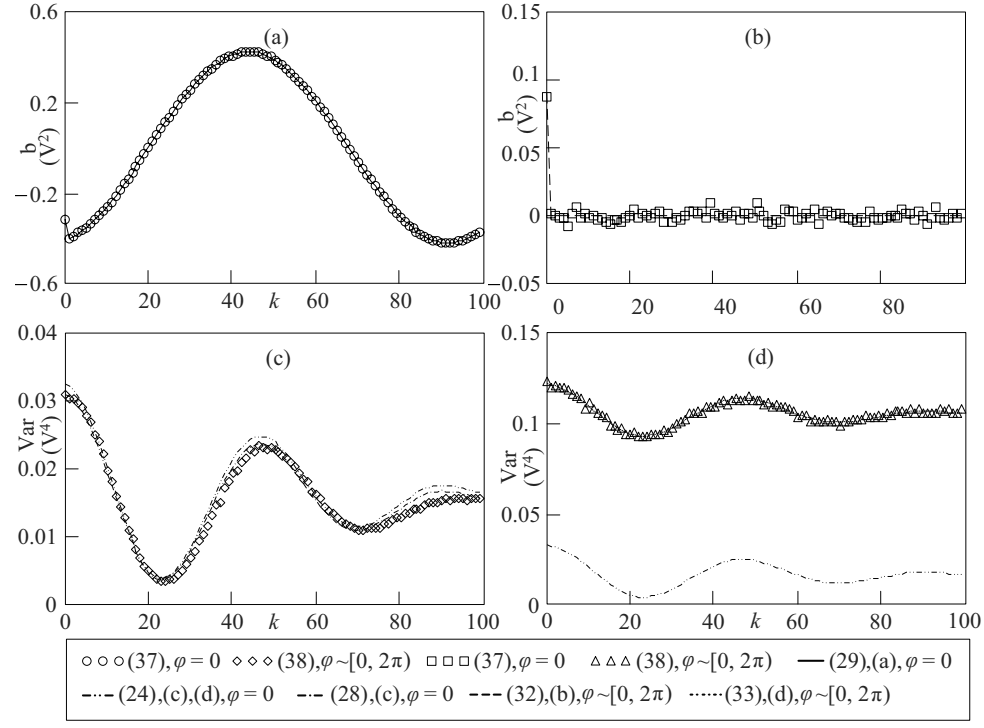

Fig. 2. Variance and bias of the ACF estimator as a function of k for $A = 3\sqrt{2}$ V, $f = 50$ Hz, $\omega = 0.021$ ($N = 2.1$), $M = 100$, SNR $= 20$ dB, and $K = 1000$: $\varphi = 0$ (a), $\varphi \sim$ U[0, 2π) (b), $\varphi = 0$ (c), and $\varphi \sim$ U[0, 2π) (d).

The error values (36) confirm the earlier conclusions (Tables 2 and 3). Equations (30) and (34) function properly in all the considered measurement situations. The greatest differences between the relative errors (30), (34), and (36) do not exceed 1 dB. Error (25) is often significantly lower than the remaining errors, but the values of error (36) prove that it is underestimated. Note that if SNR $\gg 0$, then a further increase in the SNR does not cause a decrease in the MSE. As SNR $\to \infty$ and under synchronized triggering measurement conditions, the boundary value of the error (30) amounts to

$$\mathrm{MSE}\left[\tilde{\mathrm{R}}_{\mathrm{y}}\left[k_0\right]\right] = \mathrm{MSE}\left[\tilde{\mathrm{R}}_{\mathrm{x}}\left[k_0\right]\right] = \rho^2\left(k_0\right). \tag{39}$$

When the measurement triggering is random and SNR $\to \infty$, then the boundary value of error (34) is

$$\begin{aligned}\mathrm{MSE}\left[\tilde{\mathrm{R}}_{\mathrm{y}}\left[k_0\right]\right] &= \mathrm{Var}\left[\tilde{\mathrm{R}}_{\mathrm{x}}\left[k_0\right]\right] \\ &= \frac{A^4}{16M^2}\frac{1-\cos\left(2M\omega_0\right)}{\sin^2\left(\omega_0\right)}.\end{aligned} \tag{40}$$

In the measurement situations shown in Figs. 3(a) and 3(b), the relative errors (39) and (40) are equal to –28.03 dB and –28.64 dB, respectively (c.f. the results from Tables 2 and 3 for SNR = 70 dB). Moreover, it was observed that if SNR $\gg 0$, then under the conditions of a synchronized triggering measurement and non-synchronized signal sampling, the phase φ significantly affects the MSE (Table 3, Fig. 4(d)). If the sampling is synchronized, then phase changes do not have a significant impact on the MSE (Figs. 4(a) and 4(b)).

Note that at certain points of the characteristics in Figs. 3(e) and 3(f), the relative errors (30) and (34) assume the same values as the relative error (25). This is attributed to the occurrence of synchronized sampling conditions at these points. At these points, the estimator errors are also the smallest. For example, if $\omega = 0.12$ ($N = 12$), then, relative errors (25), (30), and (34) in Figs. 3(e) and 3(f) assume a value of -84.09 dB (Table 2). In the case of the error (34), it results from the fact that $\cos(2M\omega_0) = \cos(24\pi) = 1$, whereas in the case of the error (30), from the fact that $\tilde{\mathrm{R}}_{\mathrm{x}}[0] = A^2/2 = 9\ \mathrm{V}^2$ and $\tilde{\mathrm{R}}_{\mathrm{x}}[2k_0] = (A^2/2)\cos(2k_0\omega_0) = 4.83\ \mathrm{V}^2$.

5. Experimental studies

In order to verify the formulas for the errors of the ACF estimator presented in Section 3, measurements consisting of the acquisition of the samples u[n] of a sinusoidal voltage $u(t)$ were conducted. Based on the samples u[n] and Eqn. (4), K results of the estimation of the ACF $R_u(\tau)$ ($\tilde{\mathrm{R}}_{\mathrm{u}}^{(0)}[k]$, $\tilde{\mathrm{R}}_{\mathrm{u}}^{(1)}[k]$, ..., $\tilde{\mathrm{R}}_{\mathrm{u}}^{(K-1)}[k]$) of the voltage $u(t)$ were determined. Then, the bias

$$\tilde{\mathrm{b}}\left[\tilde{\mathrm{R}}_{\mathrm{u}}\left[k\right]\right] = \frac{1}{K}\sum_{m=0}^{K-1}\tilde{\mathrm{R}}_{\mathrm{u}}^{(m)}\left[k\right] - R_u\left(\frac{k}{f_s}\right), \tag{41}$$

the variance

$$\begin{aligned}&\tilde{\mathrm{V}}\mathrm{ar}\left[\tilde{\mathrm{R}}_{\mathrm{u}}\left[k\right]\right] \\ &= \frac{1}{K}\sum_{j=0}^{K-1}\left(\frac{1}{K}\sum_{m=0}^{K-1}\tilde{\mathrm{R}}_{\mathrm{u}}^{(m)}\left[k\right] - \tilde{\mathrm{R}}_{\mathrm{u}}^{(j)}\left[k\right]\right)^2,\end{aligned} \tag{42}$$

and the mean squared error

$$\tilde{\mathrm{M}}\mathrm{SE}\left[\tilde{\mathrm{R}}_{\mathrm{u}}\left[k\right]\right] = \tilde{\mathrm{V}}\mathrm{ar}\left[\tilde{\mathrm{R}}_{\mathrm{u}}\left[k\right]\right] + \tilde{\mathrm{b}}^2\left[\tilde{\mathrm{R}}_{\mathrm{u}}\left[k\right]\right], \tag{43}$$

where

$$R_u\left(\tau\right) = \mathrm{V}_{\mathrm{RMS_{ref}}}^2\cos\left(2\pi f_{\mathrm{ref}}\tau\right), \tag{44}$$

were determined, and the error values were compared to those obtained using the formulas presented in Section 3. The quantities $\mathrm{V}_{\mathrm{RMS_{ref}}}$ and f_{ref} are, respectively, the reference voltage and the reference frequency.

The sinusoidal voltage $u(t)$ with the RMS value $\mathrm{V}_{\mathrm{RMS}} = 3$ V and the frequency value $f = 50$ Hz was generated using an Agilent 33220A function generator. The accuracy of setting the values of both parameters resulted from the function generator inaccuracy. The AC voltage was sampled using a National Instruments PCI-6024E 12 Bit data acquisition card. The sampling rate was set at $f_s = 50$ kHz. This sinusoidal signal frequency was assumed due to the limited maximum sampling frequency of the measuring card used (200 kS/s) and greater generator voltage stability in the low frequency range. The measurement results were obtained using LabVIEW. Subsequently, these measurement results were processed using MathCAD. A simple Matlab script was also written and added to MathCAD as a plug-in. This script allowed the SNR to be determined on the basis of the voltage samples.

During the experiment, no additional controlling signal was applied for measurement triggering. This implied that the studies were conducted under random triggering measurement conditions. As a result of the measurements, a file containing $K = 100$ measurement series was obtained. Each measurement series contained 5000 samples u[n]. The SNR was determined for each series. It was obtained that SNR $\in$ [$\mathrm{SNR_{min}}$, $\mathrm{SNR_{max}}$], where $\mathrm{SNR_{min}} = 67.73$ dB and $\mathrm{SNR_{max}} = 68.53$ dB. An Agilent 34401A multimeter and an AIM-TTI TF930 frequency meter (the measurement time was set at 100 s) were additionally connected to the generator. Their task was to measure the reference RMS value $\mathrm{V}_{\mathrm{RMS_{ref}}}$ and the reference frequency value f_{ref} required to determine the errors of the estimators. In the presented example, $\mathrm{V}_{\mathrm{RMS_{ref}}} = 2.9930$ V (the value of $\mathrm{V}_{\mathrm{RMS_{ref}}}$ was determined on the basis of an average of 10 measurement results), and $f_{\mathrm{ref}} = 49.9984$ Hz. The standard uncertainty of the signal sample resulting from the resolution of the data acquisition card (12 Bit) was equal to $7.05{\cdot}10^{-4}$ V, while the relative standard uncertainty of the ACF sample

Table 2. Sample relative errors defined by (25), (30), (34), and (36) corresponding to Fig. 3.

MSE [dB]	(25)	(30)	(34)	(36)	
SNR, M, ω/φ	$\varphi = 0$	$\varphi = 0$	$\varphi \sim$ U[0, 2π)	$\varphi = 0$	$\varphi \sim$ U[0, 2π)
SNR = 20 dB (Figs. 3(a) and 3(b))	–34.09	–27.10	–27.55	–27.01	–27.55
SNR = 70 dB (Figs. 3(a) and 3(b))	–84.10	–28.03	–28.64	–28.03	–28.60
$M = 100$ (Figs. 3(c) and 3(d))	–34.09	–27.10	–27.55	–27.06	–27.47
$\omega = 0.021$ ($N = 2.1$) (Figs. 3(e) and 3(f))	–84.10	–28.03	–28.64	–28.03	–28.66
$\omega = 0.12$ ($N = 12$) (Figs. 3(e) and 3(f))	–84.09	–84.09	–84.09	–84.19	–83.78

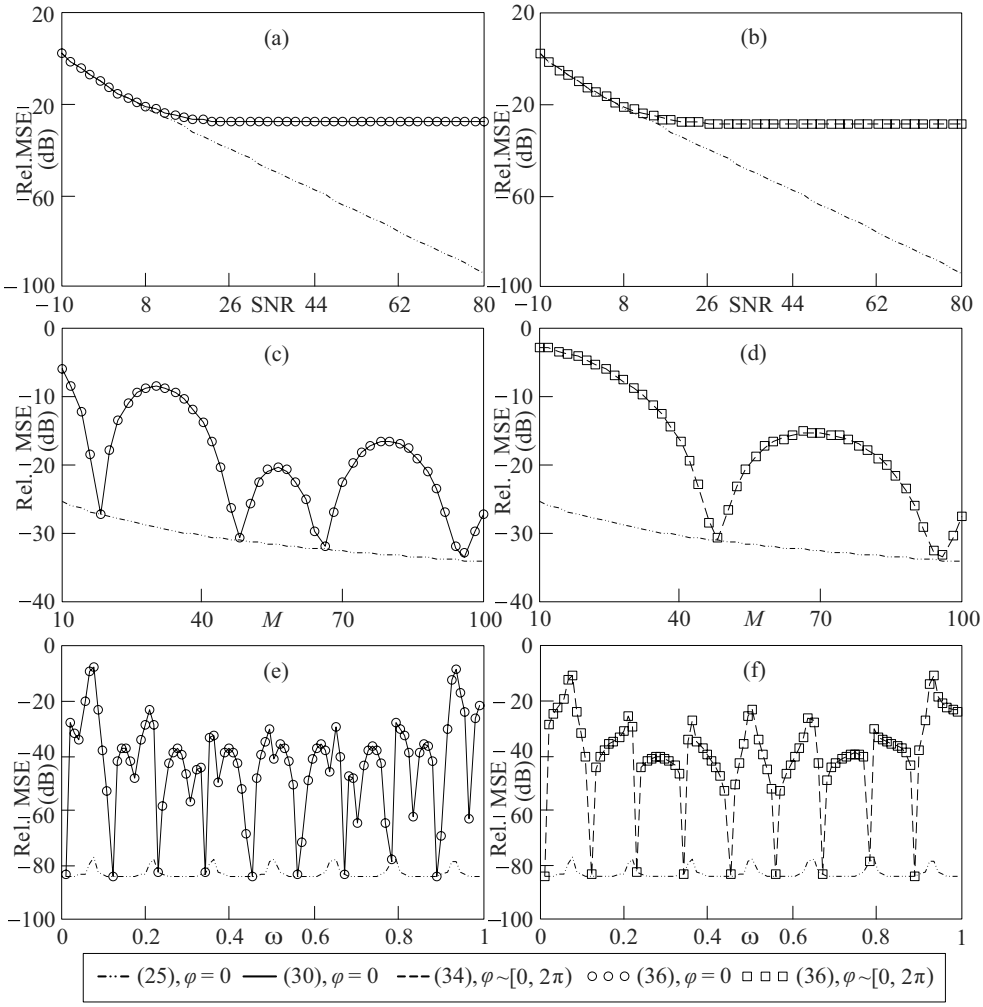

Fig. 3. Relative MSEs of the ACF estimator as a function of the SNR, M, and ω for $A = 3\sqrt{2}$ V, $f = 50$ Hz, $k_0 = 7$, and $K = 1000$: $M = 100$, $\omega = 0.021$ ($N = 2.1$), $\varphi = 0$ (a), $M = 100$, $\omega = 0.021$ ($N = 2.1$), $\varphi \sim$ U[0, 2π) (b), $\omega = 0.021$ ($N = 2.1$), SNR = 20 dB, $\varphi = 0$ (c), $\omega = 0.021$ (N =2.1), SNR = 20 dB, $\varphi \sim$ U[0, 2π) (d), $M = 100$, SNR =70 dB, $\varphi = 0$ (f), and $M = 100$, SNR = 70 dB, $\varphi \sim$ U[0, 2π) (e).

for $k = 0$ due to quantization was equal to –86.55 dB. The standard uncertainty of the voltage measurement resulting from the multimeter inaccuracy was equal to $2.78{\cdot}10^{-3}$ V, while the relative standard uncertainty of the ACF sample for $k = 0$ caused by this inaccuracy was equal to –90.27 dB. The standard uncertainty of the frequency measurement was equal to $2.89{\cdot}10^{-5}$ Hz and was mainly due to the occurrence of noise in the voltage from the generator (systematic errors of the frequency meter were negligibly small). This implied that the errors due to quantization and measurement inaccuracy were negligibly small compared with the error values (43) (see Fig. 5 and Table 5).

After taking the measurements, an operation consisting of selecting every D-th sample from each measurement series was conducted. In this way, $K = 100$ series consisting of $5000/D$ voltage samples ($M \leq 5000/(2D)$ samples per period) were obtained. Then, new values $f_s^{(D)} = f_s/D$, $\omega_0^{(D)} = 2\pi f_{\text{ref}}/f_s^{(D)}$, $N^{(D)} = M\omega_0^{(D)}/\pi$ (Table 4) and $\tilde{\text{R}}_{\text{u}}^{(0)}[k]$, $\tilde{\text{R}}_{\text{u}}^{(1)}[k]$, …, $\tilde{\text{R}}_{\text{u}}^{(K-1)}[k]$ were determined. On this basis, relative errors (25), (34), and (43) were determined (Table 5) and their diagrams (Fig. 5) were made.

The experimental studies showed that under the assumed measurement conditions, the difference between errors (34) and (43) in each of the considered cases did not exceed 1 dB (see sample results in Table 5). Similar values of errors (34) and (43) followed from the fact that both the errors depended to a greater degree on the variance (related to noise), rather than on the bias (related to systematic errors) of an ACF estimator. For example, for the results shown in Fig. 5(a) and $k = 20$, 50, 80, the squared bias (32) was equal to zero, and the squared bias (41) was equal to $1.13{\cdot}10^{-4}$ V^4, $4.07{\cdot}10^{-4}$ V^4, and $3.61{\cdot}10^{-4}$ V^4. At the same time, the variance (33) was equal to 0.062 V^4, while the variance (50) was equal to 0.058 V^4, 0.065 V^4, and 0.060 V^4. The error (34) calculated for $\text{SNR}_{\min}$ and $\text{SNR}_{\max}$ had values close to each other. A similar situation was observed in the case of the error (25), but this error was underestimated, which confirmed the results of the simulation studies. The experimental studies showed that Eqn. (34) could successfully model the actual MSE under the conditions of a random triggering measurement and non-synchronized signal sampling.

6. Conclusion

In this paper, the results of a study on the ACF estimator of a harmonic signal occurring in the presence of Gaussian noise were presented. New formulas making it possible to calculate the bias, the variance and the MSE of the ACF estimator measured under random triggering measurement conditions were designed in the reported study. Moreover, the variance of the ACF estimator of a signal measured under synchronized triggering measurement conditions known from the literature was presented.

The simulation studies confirmed the correct functioning of the designed formulas. The experimental studies showed that the new formulas could be applied to the modeling of the real errors of ACF estimators. The results showed that the difference between theoretical errors and the errors of ACF estimators calculated on the basis of signal samples did not exceed 1 dB. The presented tools enable, among other things, determination of corrections to eliminate systematic errors of the ACF estimator and minimization of MSEs as a result of appropriate selection of the number of samples and the sampling frequency for a fixed signal frequency. In addition, the values of the bias, the variance and the MSE obtained with the developed tools can be used to evaluate the statistical properties of various estimators, such as the amplitude, the frequency and the phase of harmonic and polyharmonic signals, which are built on the basis of the ACF.

Table 3. Sample relative error values (25), (30), and (36) from Figs. 4(c) and 4(d).

MSE [dB]	φ/ SNR	SNR = 20 dB	SNR = 70 dB
(25)	$\varphi = 0$	–34.09	–84.10
	$\varphi = \pi/4$	–34.09	–84.10
(30)	$\varphi = 0$	–27.10	–28.03
	$\varphi = \pi/4$	–28.05	–29.34
(36)	$\varphi = 0$	–27.02	–28.03
	$\varphi = \pi/4$	–28.01	–29.34

Table 4. Parameters of the voltage $u(t)$ processing under the conditions of a random triggering measurement and non-synchronized signal sampling.

D	M	$f_s^{(D)}$ [kHz]	$\omega_0^{(D)}/\pi$	$N^{(D)}$
24	100	50/24	24/500	24/5
49	50	50/49	49/500	49/10
99	25	50/99	99/500	99/20
249	10	50/249	249/500	249/50

Table 5. Sample relative error values (25), (34), and (43) from Fig. 5(a).

MSE [dB]	SNR/k	$k = 20$	$k = 50$	$k = 80$
(25)	$\text{SNR}_{\min}$	–82.17	–76.78	–83.14
	$\text{SNR}_{\max}$	–82.96	–77.58	–83.93
(34)	$\text{SNR}_{\min}$	–31.09	–20.97	–30.006
	$\text{SNR}_{\max}$	–31.09	–20.97	–30.01
(51)	—	–31.40	–20.74	–30.10

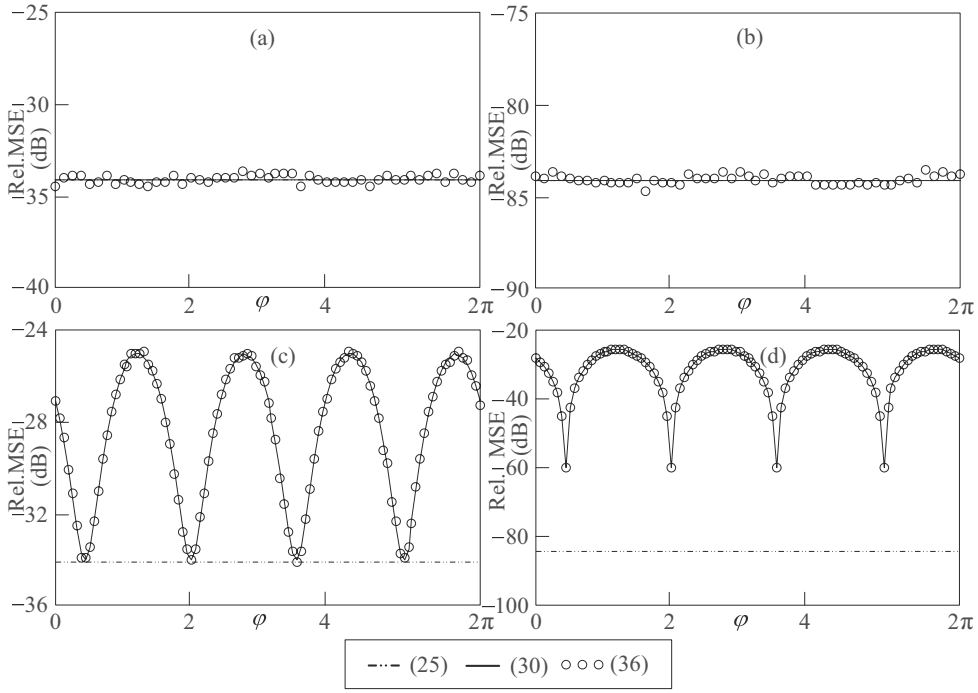

Fig. 4. Relative MSEs of the ACF estimator as a function of φ for $A = 3\sqrt{2}$ V, $f = 50$ Hz, $M = 100$, and$K = 1000$: $\omega = 0.02$ ($N = 2$), SNR $= 20$ dB (a), $\omega = 0.02$ ($N = 2$), SNR $= 70$ dB (b), $\omega = 0.021$ ($N = 2.1$), SNR $= 20$ dB (c), and $\omega = 0.021$ ($N = 2.1$), SNR $=70$ dB (d).

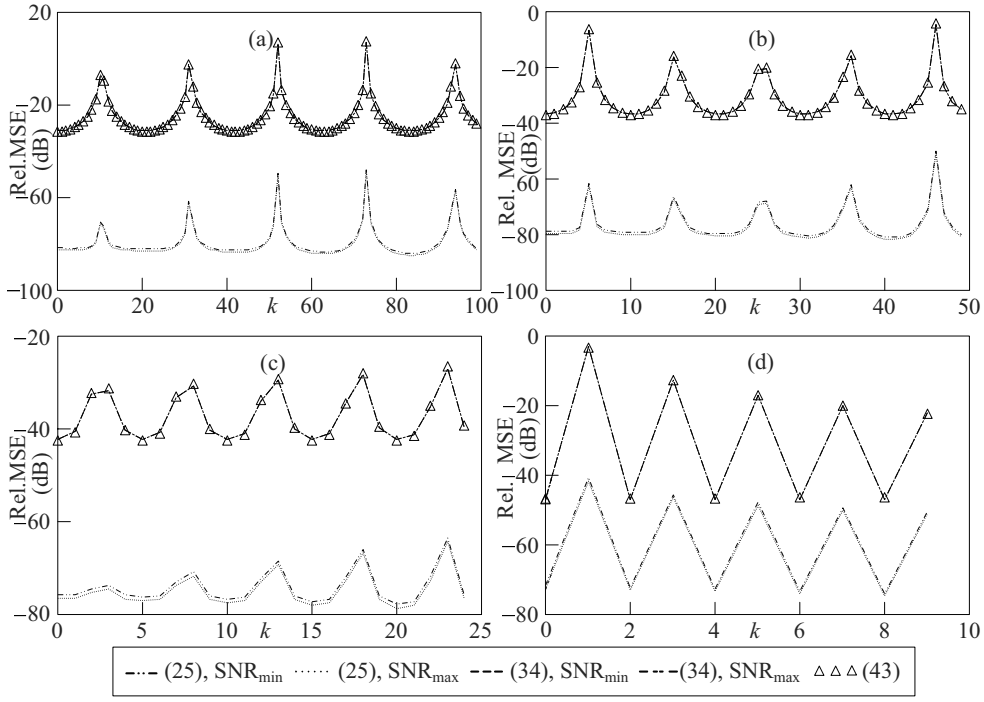

Fig. 5. Relative MSEs of the ACF estimator as a function of k for $V_{RMS} = 3$ V and $f = 50$ Hz: $M = 100$, $D = 24$ (a), $M = 50$, $D = 49$ (b), $M =25$, $D = 99$ (c), and $M = 10$, $D = 249$ (d).

References

Akkucuk, U. (2019). *Handbook of Research on Creating Sustainable Value in the Global Economy*, IGI Global, Hershey.

Al-Qudsi, B., El-Shennawy, M., Joram, N. and Ellinger, F. (2017). Enhanced zero crossing frequency estimation for FMCW radar systems, *Proceedings of the 13th Conference on PhD Research in Microelectronics and Electronics (PRIME), Taormina, Italy*, pp. 53–56.

Beck, M.S. and Plaskowski, A. (1987). *Cross Correlation Flowmeters, Their Design and Application*, Adam Hilger, Bristol.

Bendat, J.S. and Piersol, A.G. (2010). *Random Data: Analysis and Measurement Procedures, 4th Edition*, Wiley, Hoboken.

Box, G.E.P., Jenkins, G. and Reinsel, G. (2008). *Time Series Analysis: Forecasting and Control, 4th Edition*, Wiley, Hoboken.

Broersen, P.M.T. (2006). *Automatic Autocorrelation and Spectral Analysis*, Springer-Verlag, London.

Cao, Y., Wei, G. and Chen, F.-J. (2012). An exact analysis of modified covariance frequency estimation algorithm based on correlation of single-tone, *Signal Processing* **92**(11): 2785–2790.

Chen, W.-K. (2004). *The Electrical Engineering Handbook*, Academic Press, Amsterdam.

De Gooijer, J.G. and Anderson, O.D. (1985). Moments of the sampled space-time autocovariance and autocorrelation function, *Biometrika* **72**(3): 689–693.

Elasmi-Ksibi, R., Besbes, H., López-Valcarce, R. and Cherif, S. (2010). Frequency estimation of real-valued single-tone in colored noise using multiple autocorrelation lags, *Signal Processing* **90**(7): 2303–2307.

Grzegorzewski, P., Hryniewicz, O. and Romaniuk, M. (2020). Flexible resampling for fuzzy data, *International Journal of Applied Mathematics and Computer Science* **30**(2): 281–297, DOI: 10.34768/amcs-2020-0022.

Hague, D.A. and Buck, J.R. (2019). An experimental evaluation of the generalized sinusoidal frequency modulated waveform for active sonar systems, *Journal of the Acoustical Society of America* **145**(6): 3741–3755.

Hanus, R. (2019). Time delay estimation of random signals using cross-correlation with Hilbert transform, *Measurement* **146**: 792–799.

Hołyst, R., Poniewierski, A. and Zhang, X. (2017). Analytical form of the autocorrelation function for the fluorescence correlation spectroscopy, *Soft Matter* **13**(6): 1267–1275.

Hussein, H.M., Terra, O., Hussein, H. and Medhat, M. (2020). Collinear versus non-collinear autocorrelation between femtosecond pulses for absolute distance measurement, *Measurement* **152**: 107319.

Iqbal, S., Zang, X., Zhu, Y., Saad, H.M.A.A. and Zhao, J. (2015). Nonlinear time-series analysis of different human walking gaits, *Proceedings of the 2015 IEEE International Conference on Electro/Information Technology, DeKalb, USA*, pp. 25–30.

JCGM (2008). Evaluation of measurement data. guide to the expression of uncertainty in measurement, *Technical Report 100*, Joint Committee for Guides in Metrology, Sévres.

Kalvani, P.R., Jahangiri, A.R., Shapouri, S., Sari, A. and Jalili, Y.S. (2019). Multimode AFM analysis of aluminum-doped zinc oxide thin films sputtered under various substrate temperatures for optoelectronic applications, *Radio Science* **132**: 106173.

Kogan, L. (1998). Correction functions for digital correlators with two and four quantization levels, *Superlattices and Microstructures* **33**(5): 1289–1296.

Kowalczyk, A., Hanus, R. and Szlachta, A. (2016). Time delay measurement method using conditional averaging of the delayed signal module, *Przegląd Elektrotechniczny* **92**(9): 279–282.

Krajewski, M. (2018). Constructing an uncertainty budget for voltage rms measurement with a sampling voltmeter, *Metrologia* **55**(1): 95–105.

Lal-Jadziak, J. and Sienkowski, S. (2008). Models of bias of mean square value digital estimator for selected deterministic and random signals, *Metrology and Measurement Systems* **15**(1): 55–67.

Lal-Jadziak, J. and Sienkowski, S. (2009). Variance of random signal mean square value digital estimator, *Metrology and Measurement Systems* **16**(2): 267–277.

Martinez, M.A. and Ashrafi, A. (2018). Real-valued single-tone frequency estimation using half-length autocorrelation, *Digital Signal Processing* **83**: 98–106.

Menhaj, A., Assaad, J., Rouvaen, J.M., Heddebaut, M. and Bruneel, C. (1998). A new collision avoidance radar system using correlation receiver and compressed pulses, *Measurement Science and Technology* **9**(2): 283–286.

Nielsen, E. and Rietveld, M.T. (2003). Observations of backscatter autocorrelation functions from 1.07-m ionospheric irregularities generated by the European incoherent scatter heater facility, *Journal of Geophysical Research: Space Physics* **108**(A5): 1166.

Peng, J. and Boscolo, S. (2016). Filter-based dispersion-managed versatile ultrafast fibre laser, *Scientific Reports* **6**: 25995.

Pfeifer, P.E. and Deutsch, S.J. (1981). Variance of the sample space-time autocorrelation function, *Journal of the Royal Statistical Society B* **43**(1): 28–33.

Rahman, M.M., Chowdhury, M.A. and Fattah, S.A. (2018). An efficient scheme for mental task classification utilizing reflection coefficients obtained from autocorrelation function of EEG signal, *Brain Informatics* **5**: 1–12.

Rice, F., Cowley, B., Moran, B. and Rice, M. (2001). Cramer–Rao lower bounds for QAM phase and frequency estimation, *IEEE Transactions on Communications* **49**(9): 1582–1591.

Roberts, P.P. (1997). Calculating quantization correction formulae for digital correlators with digital fringe rotation, *Astronomy and Astrophysics Supplement Series* **126**(2): 379–383.

Sienkowski, S. and Kawecka, E. (2013). Probabilistic properties of sinusoidal signal autocorrelation function, *Przegląd Elektrotechniczny* **89**(11): 98–100.

Sienkowski, S. and Krajewski, M. (2018). Simple, fast and accurate four-point estimators of sinusoidal signal frequency, *Metrology and Measurement Systems* **25**(2): 359–376.

Sienkowski, S. and Krajewski, M. (2020). Single-tone frequency estimation based on reformed covariance for half-length autocorrelation, *Metrology and Measurement Systems* **27**(3): 473–493.

Spiesberger, J.L. (1996). Identifying cross-correlation peaks due to multipaths with application to optimal passive localization of transient signals and tomographic mapping of the environment, *Journal of the Acoustical Society of America* **100**(2): 910–918.

Stodółka, J., Korzewa, L., Stodółka, W. and Gambal, J. (2017). The applicability of using parameters of the autocorrelation function in the assessment of human balance during quiet bipedal stance, *Central European Journal of Sport Sciences and Medicine* **17**(1): 79–87.

Tagade, P.M. and Choi, H.-L. (2017). A dynamic bi-orthogonal field equation approach to efficient Bayesian inversion, *International Journal of Applied Mathematics and Computer Science* **27**(2): 229–243, DOI: 10.1515/amcs-2017-0016.

Toth, L. and Kocsor, A. (2003). Harmonic alternatives to sine-wave speech, *Proceedings of the 8th European Conference on Speech Communication and Technology, Geneva, Switzerland*, pp. 2073–2076.

Tu, Y.-Q. and Shen, Y.-L. (2017). Phase correction autocorrelation-based frequency estimation method for sinusoidal signal, *Signal Processing* **130**: 183–189.

Uciński, D. (2000). Optimal selection of measurement locations for parameter estimation in distributed processes, *International Journal of Applied Mathematics and Computer Science* **10**(2): 357–379.

Vaseghi, S.V. (2008). *Advanced Digital Signal Processing and Noise Reduction, 4th Edition*, Wiley, Hoboken.

Wang, K., Ding, J., Xia, Y., Liu, X., Hao, J. and Pei, W. (2018). Two high accuracy frequency estimation algorithms based on new autocorrelation-like function for noncircular/sinusoid signal, *IEICE Transactions on Fundamentals of Electronics, Communications and Computer Sciences* **101**(7): 1065–1073.

Weber, R., Faye, C., Biraud, F. and Dansou, J. (1997). Spectral detector for interference time blanking using quantized correlator, *Astronomy and Astrophysics Supplement Series* **126**(1): 161–167.

Zeitler, R. (1997). Digital correlator for measuring the velocity of solid surfaces, *IEEE Transactions on Instrumentation and Measurement* **46**(4): 803–806.

Zhang, M., Yang, Q., Chen, X. and Zhang, A. (2018). A generalized correlation theorem for LTI systems, *Journal of Physics: Conference Series* **1169**(1): 012018.

Sergiusz Sienkowski is a professor at the University of Zielona Góra, Poland. He obtained his BSc and MSc degrees from the University of Zielona Góra in 2001 and 2003, respectively. In 2011, he received a PhD in electrical engineering from the same university. His main research interests focus on signal processing, data analysis, processing of measured data, measurement systems, and evaluation of measurement uncertainty.

Mariusz Krajewski graduated from the Technical University of Zielona Góra, Poland, in 2001, receiving an MSc in digital measurement systems. In 2009, he received a PhD in electrical engineering from the Faculty of Electrical Engineering, Computer Science and Telecommunications of the University of Zielona Góra. Currently, he is an assistant professor with the same faculty, at the Institute of Metrology, Electronics and Computer Science. His research interests focus on issues related to high-precision voltage measurements, digital signal processing and determination of measurement uncertainty.

Appendix

This appendix details formulas used to obtain the expected value, the variance, and the MSE of the estimator $\tilde{\mathrm{R}}_{\mathrm{y}}[k]$ of the $R_x(\tau)$ ACF. The obtained formulas offer good quality under random triggering measurement conditions. This corresponds to a measurement situation in which the phase φ of the sinusoidal signal $x(t)$ is random in each measurement repetition.

Consider samples $\tilde{\mathrm{R}}_{\mathrm{y}}^{(0)}[k]$, …, $\tilde{\mathrm{R}}_{\mathrm{y}}^{(K-1)}[k]$ of the ACF $R_y(\tau)$ of the signal $y(t)$. Then, on the basis of (22), we can obtain

$$\begin{aligned}
&\frac{1}{K}\sum_{j=0}^{K-1}\left(\tilde{\mathrm{R}}_{\mathrm{y}}^{(j)}[k]\right)^2 \\
&\quad=\frac{1}{K}\sum_{j=0}^{K-1}\left(g^{(j)}(k)+h^{(j)}(k)\right)^2 \\
&\quad=\frac{1}{K}\sum_{j=0}^{K-1}\left(g^{(j)}(k)\right)^2+\frac{1}{K}\sum_{j=0}^{K-1}\left(h^{(j)}(k)\right)^2 \\
&\qquad+\frac{2}{K}\sum_{j=0}^{K-1}g^{(j)}(k)\,h^{(j)}(k),
\end{aligned} \tag{A1}$$

where

$$\begin{aligned}
g^{(j)}(k)&=\tilde{\mathrm{R}}_{\mathrm{x}}^{(j)}[k]+\tilde{\mathrm{R}}_{\mathrm{q}}^{(j)}[k], \\
h^{(j)}(k)&=\left(\frac{1}{M}\sum_{n=0}^{M-1}\mathrm{x}[n]\,\mathrm{q}[n+k]\right)_j \\
&\quad+\left(\frac{1}{M}\sum_{n=0}^{M-1}\mathrm{q}[n]\,\mathrm{x}[n+k]\right)_j.
\end{aligned} \tag{A2}$$

From basic algebra it follows that $\left(g^{(j)}(k)\right)^2 + \left(h^{(j)}(k)\right)^2 \geq 2g^{(j)}(k)\,h^{(j)}(k)$. If the SNR is sufficiently large (SNR $\gg 0$), then for almost every $k \geq 0$, $\left(g^{(j)}(k)\right)^2 + \left(h^{(j)}(k)\right)^2 \gg 2g^{(j)}(k)\,h^{(j)}(k)$. This implies

$$\frac{1}{K}\sum_{j=0}^{K-1}\left(g^{(j)}(k)\right)^2 + \frac{1}{K}\sum_{j=0}^{K-1}\left(h^{(j)}(k)\right)^2 \gg \frac{2}{K}\sum_{j=0}^{K-1} g^{(j)}(k)\,h^{(j)}(k). \quad \text{(A3)}$$

Thus,

$$\frac{1}{K}\sum_{j=0}^{K-1}\left(\tilde{\mathrm{R}}_{\mathrm{y}}^{(j)}[k]\right)^2 \approx \frac{1}{K}\sum_{j=0}^{K-1}\left(g^{(j)}(k)\right)^2 + \frac{1}{K}\sum_{j=0}^{K-1}\left(h^{(j)}(k)\right)^2. \quad \text{(A4)}$$

Let us first consider the case where $k = 0$. The first term of the sum in (A.4) then assumes the form

$$\frac{1}{K}\sum_{j=0}^{K-1}\left(g^{(j)}(0)\right)^2 = \frac{1}{K}\sum_{j=0}^{K-1}\left(\tilde{\mathrm{R}}_{\mathrm{x}}^{(j)}[0]\right)^2 + \frac{2}{K}\sum_{j=0}^{K-1}\tilde{\mathrm{R}}_{\mathrm{x}}^{(j)}[0]\,\tilde{\mathrm{R}}_{\mathrm{q}}^{(j)}[0] + \frac{1}{K}\sum_{j=0}^{K-1}\left(\tilde{\mathrm{R}}_{\mathrm{q}}^{(j)}[0]\right)^2. \quad \text{(A5)}$$

The phase $\varphi^{(j)}$ affects the component $\rho^{(j)}(0)$ in (9) such that

$$\frac{1}{K}\sum_{j=0}^{K-1}\tilde{\mathrm{R}}_{\mathrm{x}}^{(j)}[0] = \frac{A^2}{2} + \frac{1}{K}\sum_{j=0}^{K-1}\rho^{(j)}(0) \approx \frac{A^2}{2}. \quad \text{(A6)}$$

Since

$$\tilde{\mathrm{R}}_{\mathrm{q}}^{(0)}[0] \approx \cdots \approx \tilde{\mathrm{R}}_{\mathrm{q}}^{(K-1)}[0] \approx \tilde{\mathrm{R}}_{\mathrm{q}}[0] \approx \sigma_q^2, \quad \text{(A7)}$$

we get

$$\frac{1}{K}\sum_{j=0}^{K-1}\tilde{\mathrm{R}}_{\mathrm{x}}^{(j)}[0]\,\tilde{\mathrm{R}}_{\mathrm{q}}^{(j)}[0] \approx \frac{A^2}{2}\sigma_q^2. \quad \text{(A8)}$$

Moreover,

$$\begin{aligned}\frac{1}{K}\sum_{j=0}^{K-1}&\left(\tilde{\mathrm{R}}_{\mathrm{x}}^{(j)}[0]\right)^2 = \frac{1}{K}\sum_{j=0}^{K-1}\left(\frac{A^2}{2} + \rho^{(j)}(0)\right)^2 \\ &\approx \frac{A^4}{4} + \frac{A^4}{16M^2\sin^2(\omega_0)}\frac{1}{K}\sum_{j=0}^{K-1}\left(\sin\left(2\varphi^{(j)} - \omega_0\right)\right. \\ &\quad \left. - \sin\left((2M-1)\omega_0 + 2\varphi^{(j)}\right)\right)^2 \\ &\approx \frac{A^4}{4} + \frac{A^4}{16M^2}\frac{1-\cos(2M\omega_0)}{\sin^2(\omega_0)}.\end{aligned} \quad \text{(A9)}$$

Therefore,

$$\frac{1}{K}\sum_{j=0}^{K-1}\left(g^{(j)}(0)\right)^2 \approx \frac{A^4}{16M^2}\frac{1-\cos(2M\omega_0)}{\sin^2(\omega_0)} + \frac{A^4}{4} + A^2\sigma_q^2 + \frac{M+2}{M}\sigma_q^4. \quad \text{(A10)}$$

Since we have (Martinez and Ashrafi, 2018)

$$\frac{1}{K}\sum_{j=0}^{K-1}\left(\left(\frac{1}{M}\sum_{n=0}^{M-1}\mathrm{x}[n]\,\mathrm{q}[n]\right)_j\right)^2 \approx \frac{\sigma_q^2}{M}\tilde{\mathrm{R}}_{\mathrm{x}}[0], \quad \text{(A11)}$$

for $k = 0$ the second term in (A.4) reduces to

$$\begin{aligned}\frac{1}{K}\sum_{j=0}^{K-1}&\left(h^{(j)}(0)\right)^2 = \frac{4}{K}\sum_{j=0}^{K-1}\left(\left(\frac{1}{M}\sum_{n=0}^{M-1}\mathrm{x}[n]\,\mathrm{q}[n]\right)_j\right)^2 \\ &\approx \frac{2}{M}A^2\sigma_q^2.\end{aligned} \quad \text{(A12)}$$

Thus,

$$\begin{aligned}\frac{1}{K}\sum_{j=0}^{K-1}&\left(\tilde{\mathrm{R}}_{\mathrm{y}}^{(j)}[0]\right)^2 \approx \frac{A^4}{16M^2}\frac{1-\cos(2M\omega_0)}{\sin^2(\omega_0)} \\ &+ \frac{A^4}{4} + \left(1+\frac{2}{M}\right)A^2\sigma_q^2 + \frac{M+2}{M}\sigma_q^4.\end{aligned} \quad \text{(A13)}$$

Simultaneously,

$$\frac{1}{K}\sum_{j=0}^{K-1}\tilde{\mathrm{R}}_{\mathrm{y}}^{(j)}[0] \approx \frac{A^2}{2} + \sigma_q^2. \quad \text{(A14)}$$

This implies that for $k = 0$, the expected value and variance of the estimator $\tilde{\mathrm{R}}_{\mathrm{y}}[k]$ can be expressed as follows:

$$\begin{aligned}\mathrm{E}\left[\tilde{\mathrm{R}}_{\mathrm{y}}[k]\right] &= \frac{A^2}{2} + \sigma_q^2,\\ \mathrm{Var}\left[\tilde{\mathrm{R}}_{\mathrm{y}}[k]\right] &= \frac{A^4}{4} + \frac{A^4}{16M^2}\frac{1-\cos(2M\omega_0)}{\sin^2(\omega_0)}\\ &\quad + A^2\sigma_q^2\left(1+\frac{2}{M}\right) + \frac{M+2}{M}\sigma_q^4\\ &\quad - \left(\frac{A^2}{2} + \sigma_q^2\right)^2\\ &= \frac{A^4}{16M^2}\frac{1-\cos(2M\omega_0)}{\sin^2(\omega_0)} + \frac{2\sigma_q^4}{M} + \frac{2A^2\sigma_q^2}{M}.\end{aligned} \tag{A15}$$

Consider the case of $k > 0$. The first term of the sum in (A.4) then has the form

$$\begin{aligned}\frac{1}{K}\sum_{j=0}^{K-1}\left(g^{(j)}(k)\right)^2 &= \frac{1}{K}\sum_{j=0}^{K-1}\left(\tilde{\mathrm{R}}_{\mathrm{x}}^{(j)}[k]\right)^2\\ &\quad + \frac{2}{K}\sum_{j=0}^{K-1}\tilde{\mathrm{R}}_{\mathrm{x}}^{(j)}[k]\,\tilde{\mathrm{R}}_{\mathrm{q}}^{(j)}[k]\\ &\quad + \frac{1}{K}\sum_{j=0}^{K-1}\left(\tilde{\mathrm{R}}_{\mathrm{q}}^{(j)}[k]\right)^2.\end{aligned} \tag{A16}$$

Similarly, as in (A.6)–(A.9), we obtain

$$\begin{aligned}\frac{1}{K}\sum_{j=0}^{K-1}\tilde{\mathrm{R}}_{\mathrm{x}}^{(j)}[k] &= \frac{A^2}{2}\cos(k\omega_0) + \frac{1}{K}\sum_{j=0}^{K-1}\rho^{(j)}(k)\\ &\approx \frac{A^2}{2}\cos(k\omega_0),\end{aligned} \tag{A17}$$

$$\begin{aligned}&\frac{1}{K}\sum_{j=0}^{K-1}\left(\tilde{\mathrm{R}}_{\mathrm{x}}^{(j)}[k]\right)^2\\ &\quad = \left(\frac{A^2}{2}\cos(k\omega_0) + \frac{1}{K}\sum_{j=0}^{K-1}\rho^{(j)}(k)\right)^2\\ &\quad \approx \frac{A^4}{4}\cos^2(k\omega_0) + \frac{A^4}{16M^2}\frac{1-\cos(2M\omega_0)}{\sin^2(\omega_0)}.\end{aligned} \tag{A18}$$

On the basis of

$$\frac{1}{K}\sum_{j=0}^{K-1}\tilde{\mathrm{R}}_{\mathrm{q}}^{(j)}[k] \approx 0, \qquad \frac{1}{K}\sum_{j=0}^{K-1}\left(\tilde{\mathrm{R}}_{\mathrm{q}}^{(j)}[k]\right)^2 \approx \frac{\sigma_q^4}{M}, \tag{A19}$$

and (A.16)–(A.18), we can obtain

$$\begin{aligned}\frac{1}{K}\sum_{j=0}^{K-1}\left(g^{(j)}(k)\right)^2 &\approx \frac{A^4}{4}\cos^2(k\omega_0)\\ &\quad + \frac{A^4}{16M^2}\frac{1-\cos(2M\omega_0)}{\sin^2(\omega_0)} + \frac{\sigma_q^4}{M}.\end{aligned} \tag{A20}$$

The second term of the sum in formula (A.4) then takes the form

$$\begin{aligned}&\frac{1}{K}\sum_{j=0}^{K-1}\left(h^{(j)}(k)\right)^2\\ &\quad = \frac{1}{K}\sum_{j=0}^{K-1}\left(\left(\frac{1}{M}\sum_{n=0}^{M-1}\mathrm{x}[n]\,\mathrm{q}[n+k]\right)_j\right)^2\\ &\quad + \frac{1}{K}\sum_{j=0}^{K-1}\left(\left(\frac{1}{M}\sum_{n=0}^{M-1}\mathrm{q}[n]\,\mathrm{x}[n+k]\right)_j\right)^2\\ &\quad + \frac{2}{K}\sum_{j=0}^{K-1}\left\{\left(\frac{1}{M}\sum_{n=0}^{M-1}\mathrm{x}[n]\,\mathrm{q}[n+k]\right)_j\right.\\ &\quad \left.\cdot\left(\frac{1}{M}\sum_{n=0}^{M-1}\mathrm{q}[n]\,\mathrm{x}[n+k]\right)_j\right\}.\end{aligned} \tag{A21}$$

When

$$\begin{aligned}&\frac{1}{K}\sum_{j=0}^{K-1}\left(\left(\frac{1}{M}\sum_{n=0}^{M-1}\mathrm{x}[n]\,\mathrm{q}[n+k]\right)_j\right)^2\\ &\quad \approx \frac{A^2\sigma_q^2}{2M},\\ &\frac{1}{K}\sum_{j=0}^{K-1}\left(\left(\frac{1}{M}\sum_{n=0}^{M-1}\mathrm{q}[n]\,\mathrm{x}[n+k]\right)_j\right)^2\\ &\quad \approx \frac{A^2\sigma_q^2}{2M},\\ &\frac{1}{K}\sum_{j=0}^{K-1}\left\{\left(\frac{1}{M}\sum_{n=0}^{M-1}\mathrm{x}[n]\,\mathrm{q}[n+k]\right)_j\right.\\ &\quad \left.\cdot\left(\frac{1}{M}\sum_{n=0}^{M-1}\mathrm{q}[n]\,\mathrm{x}[n+k]\right)_j\right\}\\ &\quad \approx \frac{A^2\sigma_q^2}{2M^2}(M-k)\cos(2k\omega_0),\end{aligned} \tag{A22}$$

then

$$\frac{1}{K}\sum_{j=0}^{K-1}\left(h^{(j)}\left(k\right)\right)^2 \approx \frac{A^2\sigma_q^2}{M}+\frac{A^2\sigma_q^2}{M^2}\left(M-k\right)\cos\left(2k\omega_0\right). \quad \text{(A23)}$$

Therefore,

$$\begin{aligned}\frac{1}{K}\sum_{j=0}^{K-1}\left(\tilde{\mathrm{R}}_{\mathrm{y}}^{(j)}\left[k\right]\right)^2 &\approx \frac{A^4}{4}\cos^2\left(k\omega_0\right)+\frac{A^4}{16M^2}\frac{1-\cos\left(2M\omega_0\right)}{\sin^2\left(\omega_0\right)} \\ &+\frac{\sigma_q^4}{M}+\frac{A^2\sigma_q^2}{M}+\frac{A^2\sigma_q^2}{M^2}\left(M-k\right)\cos\left(2k\omega_0\right).\end{aligned} \quad \text{(A24)}$$

Simultaneously,

$$\frac{1}{K}\sum_{j=0}^{K-1}\tilde{\mathrm{R}}_{\mathrm{y}}^{(j)}\left[k\right]\approx\frac{A^2}{2}\cos\left(k\omega_0\right). \quad \text{(A25)}$$

This implies that for $k>0$, the expected value and the variance of the estimator $\tilde{\mathrm{R}}_{\mathrm{y}}[k]$ can be expressed as

$$\begin{aligned}\mathrm{E}\left[\tilde{\mathrm{R}}_{\mathrm{y}}\left[k\right]\right] &= \frac{A^2}{2}\cos\left(k\omega_0\right), \\ \mathrm{Var}\left[\tilde{\mathrm{R}}_{\mathrm{y}}\left[k\right]\right] &= \frac{A^4}{16M^2}\frac{1-\cos\left(2M\omega_0\right)}{\sin^2\left(\omega_0\right)} \\ &+\frac{A^2\sigma_q^2}{M^2}\left(M-k\right)\cos\left(2k\omega_0\right) \\ &+\frac{\sigma_q^4}{M}+\frac{A^2\sigma_q^2}{M}.\end{aligned} \quad \text{(A26)}$$

Finally, based on (A.15) and (A.26), we obtain

$$\mathrm{E}\left[\tilde{\mathrm{R}}_{\mathrm{y}}\left[k\right]\right]=\begin{cases}\dfrac{A^2}{2}+\sigma_q^2, & k=0,\\ \dfrac{A^2}{2}\cos\left(k\omega_0\right), & k>0,\end{cases} \quad \text{(A27)}$$

$$\begin{aligned}&\mathrm{Var}\left[\tilde{\mathrm{R}}_{\mathrm{y}}\left[k\right]\right] \\ &=\begin{cases}\dfrac{A^4}{16M^2}\dfrac{1-\cos\left(2M\omega_0\right)}{\sin^2\left(\omega_0\right)} & \\ +\dfrac{2\sigma_q^4}{M}+\dfrac{2A^2\sigma_q^2}{M}, & k=0,\\ \dfrac{A^4}{16M^2}\dfrac{1-\cos\left(2M\omega_0\right)}{\sin^2\left(\omega_0\right)} & \\ +\dfrac{A^2\sigma_q^2}{M^2}\left(M-k\right)\cos\left(2k\omega_0\right) & \\ +\dfrac{\sigma_q^4}{M}+\dfrac{A^2\sigma_q^2}{M}, & k>0.\end{cases}\end{aligned} \quad \text{(A28)}$$

Note that, as SNR $\to\infty$, we get

$$\begin{aligned}\mathrm{E}\left[\tilde{\mathrm{R}}_{\mathrm{x}}\left[k\right]\right] &= \frac{A^2}{2}\cos\left(k\omega_0\right), \\ \mathrm{Var}\left[\tilde{\mathrm{R}}_{\mathrm{x}}\left[k\right]\right] &= \frac{A^4}{16M^2}\frac{1-\cos\left(2M\omega_0\right)}{\sin^2\left(\omega_0\right)}.\end{aligned} \quad \text{(A29)}$$

Received: 31 May 2021
Revised: 5 September 2021
Accepted: 4 October 2021